# On the Performance of Alternative 5G Micro-Operator Deployments in 3.6 GHz and 26 GHz Bands

K. B. Shashika Manosha, K. Hiltunen†, M. Matinmikko-Blue, and M. Latva-aho
Centre for Wireless Communications, University of Oulu, Finland
†Ericsson Research, Oy L M Ericsson Ab, Finland
{manosha.kapuruhamybadalge, marja.matinmikko, matti.latva-aho}@oulu.fi
kimmo.hiltunen@ericsson.com

***Abstract*—The fifth generation (5G) networks will increasingly target specific indoor deployments such as closed factory premises or open shopping malls for local providing of high-quality services. Local 5G network operator models, such as the newly proposed micro-operators, have gained increasing interest with guaranteed quality-of-service delivery, in spatially confined areas, especially inside the buildings. However, establishing local 5G networks with quality guarantees requires local spectrum access rights which are in the agendas of many national regulators. In this paper, we study the feasibility of indoor deployment of local 5G networks in two new 5G bands including 3.6 GHz and 26 GHz. We consider different deployment alternatives for a local 5G micro-operator in the bands with different antenna configurations and network densities. Then, we evaluate the impact of the different deployments on the performance of users via system level simulations of the average and cell-edge throughputs in downlink and uplink. Numerically, we have observed that the performance achieved in these two bands can be improved by increasing the base station (BS) density of the network. Furthermore, we have seen that the centre frequency does not significantly impact on the downlink performance unless the network is noise-limited. However, the uplink performance in the 26 GHz band is affected by the higher coupling losses between the BSs and the mobile terminals. We have also noticed that beamforming and wider channel bandwidths are useful for improving the network performance in 26 GHz band.**

***Index Terms*—5G, micro operator, radio network performance, beamforming, 3.6 GHz band, 26 GHz band, system level simulations**

## I. Introduction

The fifth generation (5G) networks are expected to be the key enabler for digitalization of a diverse set of use cases [1]. There is common agreement on the use cases including massive machine type communications, critical machine type communications, and enhanced mobile broadband [2]. Serving these use cases is challenged by their inherent requirements, such as guaranteed quality-of-service levels (e.g., reliability and latency), enabling own management functionalities, and specific security standards [3].

While prior generations of mobile communication systems targeted wide area networks, the development of *local high-quality wireless networks* has started in standardization to allow the establishment of local 5G networks by different stakeholders [3], [4]. Such a network is expected to support the stringent quality-of-service (QoS) levels, privacy and security, and moreover, its operation is restricted to a spatially confined region. In line with [3] and [4], the study in [5] has demonstrated that the QoS requirements related to the 5G use cases can be achieved by densified indoor networks. However, the question becomes who will deploy these local indoor networks, which in turn will heavily depend on the availability of suitable spectrum bands for local operations with quality guarantees.

Different stakeholders especially in vertical sectors have expressed growing interest to deploy their own 5G networks, which was the main driver in the development of the micro-operator concept [6], [7]. A micro-operator is a local specific service provider that complements mobile network operators' (MNOs) offerings by providing context related services and content locally. As the micro-operators are expected to provide versatile high-quality services, their operations is crucially dependent on local access to the spectrum with no or very limited harmful interference. Some regulators are in the process of defining local licensing models discussed in [8] for assigning local access rights [9] with an appropriate spectrum authorization framework [10]. On the other hand, the harmful interference between two micro-operators can also be avoided by using an appropriate separation distance between them [11]. For protecting possible incumbents in the band, methods based on an extension of the licensed shared access (LSA) for granting local access rights are under investigation [4]. All these works highlight the importance of guaranteed access to the spectrum to enable a large number local high-quality wireless networks.

The first 5G network deployments are taking place in 700 MHz, 3.6 GHz, and 26 GHz bands in Europe [12]. While the 700 MHz band is mostly used for outdoor macro cellular deployments, the 3.6 GHz band is suitable for both outdoor and indoor networks. On the other hand, the 26 GHz band will mainly be used for local networks including indoor deployments. Hence, by looking at the requirements of local 5G networks (e.g., localized deployment and guaranteed QoS), it is clear that both 3.6 GHz and 26 GHz are potential bands for such networks.

For efficient design and deployment of a wireless network, it is necessary to define the suitable technical requirements

such as the operating band, channel bandwidth, BS type (omnidirectional or beamformed), etc. Then, an investigation is needed to identify the best combination of the above technical requirements that give the optimum performance of a network, i.e., the best deployment alternative. In the case of a local high-quality network also such an investigation is essential and useful. However, to the best of our knowledge, none of the existing studies on upcoming 5G bands have investigated the different deployment alternatives for a local 5G micro-operator network, and have not evaluated the impact of the deployment on the performance of the network.

In this paper, we study local 5G micro-operator networks deployed within a floor of a building using either 3.6 GHz or 26 GHz band. We consider three different indoor deployment alternatives with different antenna configurations. We then evaluate the performance of the network via system level simulations using average and cell-edge throughputs in downlink and uplink as the performance measures. We specifically evaluate the impact of BS densification on the performance of the local 5G network.

The main contributions of this paper are as follows:

- We study the performance of local 5G networks operating in the new 5G bands 3.6 GHz and 26 GHz for delivering local high-quality services for the indoor users.
- We quantify the benefits of beamforming and larger channel bandwidths on the performance of a local indoor 5G network operating in the 26 GHz and 3.6 GHz bands.

The rest of the paper is organized as follows. Section II introduces the system model, including the assumed network layout, propagation models and models for the radio resource management and user performance. Then, system simulation results are presented and analyzed in Section III. Finally, some conclusions are given in Section IV.

## II. System Model

In this section, we first introduce the network layout for a single indoor 5G micro-operator deployment. We then present the considered propagation model and the applied radio resource management scheme.

### A. Network Layout

We consider a single micro-operator network, deployed in a single floor of a building with dimensions $50 \times 120$ m, as shown in Fig. 1 operating either in 3.6 GHz or 26 GHz band. The BS density within the floor is varied, and the BSs are deployed so that a roughly uniform coverage can be obtained throughout the floor area. Furthermore, we assume that the BSs have either beamformed or omnidirectional antennas, and the mobile terminals have omnidirectional antennas.

### B. Propagation Model

Since the micro-operator network is deployed inside a building, we consider only an indoor propagation model. We denote the absolute value of the coupling loss between the BS $b$ and the mobile terminal $m$ on beam $n$ as $C_{mbn}$ and that

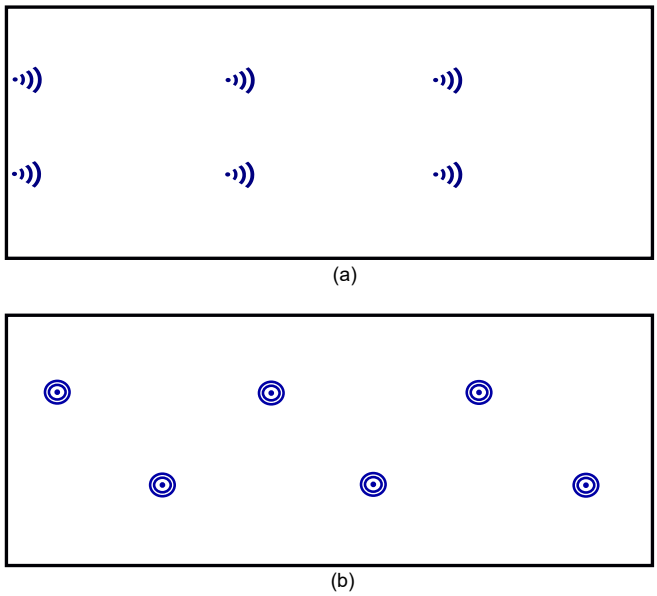


Fig. 1. Base station deployment in a single floor of a micro operator network: (a) with beamformed antennas (b) with omnidirectional antennas.

in decibel scale as $C_{mbn,\mathrm{dB}}$. The coupling loss is obtained from

$$C_{mbn,\mathrm{dB}} = L_{mb} - G_m^{\mathrm{ant}} - G_{bn}^{\mathrm{ant}} + X_{mb}, \tag{1}$$

where $L_{mb}$ is the path loss between mobile terminal $m$ and BS $b$, $G_m^{\mathrm{ant}}$ is the antenna gain of mobile terminal $m$, $G_{bn}^{\mathrm{ant}}$ is the antenna gain of BS $b$ on beam $n$, and $X_{mb}$ denotes the log-normally distributed random value that models the impact of shadowing between mobile terminal $m$ and BS $b$.

The mobile terminal antenna is assumed to be omnidirectional with antenna gain equal to 0 dBi. The base station antennas are assumed to be either omnidirectional or beamformed. In the case of omnidirectional antennas, the antenna gain is assumed to be equal to 5 dBi. In the case of beamformed base station antennas, we assume that the base station antenna consists of $4 \times 16$ cross-polarized antenna elements. Furthermore, analog beamforming is applied so that a grid of 48 different candidate beams are generated. These beams are generated within the range of approximately $\pm 55$ degrees in azimuth and $\pm 13$ degrees in elevation. The half-power beam width of each beam is approximately 8 degrees and the maximum antenna gain is equal to 23 dBi.

The indoor propagation within the floor is modeled based on 3GPP Indoor-Mixed Office propagation model defined in [13]. The path loss consists of both line-of-sight (LOS) and non-line-of-site (NLOS) components, and they are given by

$$L_{\mathrm{LOS}} = 32.4 + 17.3 \log_{10}(d_{3D}) + 20 \log_{10}(f_c), \tag{2a}$$
$$L_{\mathrm{NLOS}} = \max(L_{\mathrm{LOS}}, L'_{\mathrm{NLOS}}), \tag{2b}$$
$$L'_{\mathrm{NLOS}} = 17.3 + 38.3 \log_{10}(d_{3D}) + 24.9 \log_{10}(f_c), \tag{2c}$$

where $d_{3D}$ is the three-dimensional distance between the BS and the mobile terminal in meters and $f_c$ is the centre

frequency in GHz. The LOS probability is given by

$$P_{\mathrm{LOS}} = \begin{cases} 1 & d_{2D} \leq 1.2 \\ \exp(-\frac{d_{2D}-1.2}{4.7}) & 1.2 < d_{2D} \leq 6.5 \\ 0.32\exp(-\frac{d_{2D}-6.5}{32.6}) & d_{2D} > 6.5, \end{cases} \quad (3)$$

where $d_{2D}$ is the two-dimensional distance between the BS and the mobile terminal. While modeling the impact of shadow fading, we assume that the standard deviation is equal to 3 dB in the case of LOS and 8 dB in the case of NLOS. Furthermore, we assume that the shadow fading and the LOS probability are spatially correlated with correlation distances equal to 10 m or 6 m (shadow fading in LOS or NLOS) and 10 m (LOS probability) [13].

### C. Radio Resource Management

Our system model assumes that a user is served by only one BS using a single beam. The serving BS and the beam are chosen based on the coupling loss between the BS and the user terminal on that beam. We consider a round-robin scheduler operating in the time domain for scheduling users in both downlink (DL) and uplink (UL). We assume that the network is applying time-division-duplex (TDD); the DL and UL slots are randomly selected to have a $50:50$ ratio in average. Furthermore, we assume that the BSs in the network are synchronized, which means that the DL and UL transmission do not overlap.

The DL signal-to-interference-plus-noise ratio (SINR) of mobile terminal $m$ associated with BS $b$ on beam $n$ can be expressed as

$$\gamma_{mbn}^{\mathrm{DL}} = \frac{P_b^{\mathrm{BS}}}{C_{mbn}\left(I_{mb}+N_m\right)}, \quad (4)$$

where $P_b^{\mathrm{BS}}$ is the transmit power of $b$th BS, $N_m$ is the thermal noise power of $m$th mobile terminal, $C_{mbn}$ is the coupling loss between mobile terminal $m$ and BS $b$ on beam $n$. Notation $I_{mb}$ denotes the average inter-cell interference generated towards $m$th user of BS $b$ from all the other BSs in the network. If beamformed antennas are used at the BSs, the interference $I_{mb}$ can be expressed as

$$I_{mb} = \sum_{\substack{j=1 \\ j\neq b}}^{J} \sum_{r=1}^{48} \frac{P_j^{\mathrm{BS}}\tau_{jr}}{C_{mjr}}, \quad (5)$$

where $\tau_{jr}$ is an activity factor that indicates the probability (i.e., the average fraction of time) that beam $r$ of BS $j$ is being transmitted. For the BSs with omnidirectional antennas, the interference $I_{mb}$ is given by

$$I_{mb} = \sum_{\substack{j=1 \\ j\neq b}}^{J} \frac{P_j^{\mathrm{BS}}\tau_j}{C_{mj}}. \quad (6)$$

The uplink SINR of mobile terminal $m$ served by BS $b$ on beam $n$ is given by

$$\gamma_{mbn}^{\mathrm{UL}} = \frac{P_{mbn}^{\mathrm{MT}}}{C_{mbn}\left(\sum\limits_{\substack{j=1 \\ j\neq b}}^{J}\sum\limits_{s=1}^{u_j}\frac{P_{sj}^{\mathrm{MT}}\tau_{sj}}{C_{sbn}}+N_b\right)}, \quad (7)$$

where $P_{mbn}^{\mathrm{MT}}$ is the total transmission power of mobile terminal $m$ associated with BS $b$ on $n$th beam, $u_j$ is the set of uplink users associated with BS $j$, and $\tau_{sj}$ is an activity factor that indicates the probability of $s$th user of BS $j$ being scheduled for uplink transmission, $N_b$ is the thermal noise power of $b$th BS. The expression for $P_{mbn,\mathrm{dB}}^{\mathrm{MT}}$ (i.e.,the decibel value of $P_{mbn}^{\mathrm{MT}}$) is given by

$$P_{mbn,\mathrm{dB}}^{\mathrm{MT}} = P_b^0 + 10\log_{10}(\beta) + \alpha_b C_{mbn,\mathrm{dB}}, \quad (8a)$$

$$P_{\min}^{\mathrm{MT}} \leq P_{mbn}^{\mathrm{MT}} \leq P_{\max}^{\mathrm{MT}}, \quad (8b)$$

where $P_b^0$ is the target for the received UL power at $b$th BS, $\beta$ is the channel bandwidth, and $\alpha_b$ is the path loss compensation factor. The notations $P_{\min}^{\mathrm{MT}}$ and $P_{\max}^{\mathrm{MT}}$ define the minimum and maximum transmit powers of the mobile terminal, respectively.

The SINR values can be mapped to corresponding user throughput by using the following expression

$$R_{mb} = \frac{0.8\eta\beta\min\left(R_{\max}, \log_2(1+\gamma_{mb})\right)}{u_b}, \quad (9)$$

where $\gamma_{mb} = \gamma_{mbn}^{\mathrm{DL}}$ for the downlink and $\gamma_{mb} = \gamma_{mbn}^{\mathrm{UL}}$ for the uplink. We assume that the average overhead due to control channels and data retransmissions is equal to $20\%$. Parameter $\eta$ is used to indicate the average usage of DL and UL as a fraction of time. The maximum spectral efficiency $R_{\max}$ is defined by both the highest available modulation and coding rate and the maximum number of parallel data streams for each link. Furthermore, the the effect of round-robin scheduling is taken into account via parameter $u_b$. Finally, if $\gamma_{mb} < -10$ dB we assume that $R_{mb} = 0$, otherwise $R_{mb}$ is calculated by using (9).

## III. Evaluation Results

In this section, we evaluate the performance of a single 5G micro operator network operating in the two frequency bands 3.6 GHz and 26 GHz. We consider three deployment alternatives: 1) 3.6 GHz with omnidirectional BS antennas, 2) 26 GHz with omnidirectional BS antennas and 3) 26 GHz with beamformed BS antennas. Furthermore, for 3.6 GHz band, we assume that the channel bandwidth is 50 MHz, while for the 26 GHz band both 50 MHz and 200 MHz channel bandwidths are assumed. Other main parameters are as listed in Table I. For each deployment alternative, we numerically evaluate the average throughput and the worst fifth percentile (cell-edge) throughput in both DL and UL, by varying the BS density, while keeping total number of users unchanged.

Fig. 2 shows the normalized average DL throughput and Fig. 3 shows normalized cell-edge DL throughput versus the BS density for the different deployment alternatives. The results have been normalized with respect to the deployment that has 12 BSs in the 3.6 GHz band.

Results show that the average and cell-edge DL throughputs increase when the BS density is increased. As the BS density increases, the coupling losses from the mobile terminals towards the serving BSs become smaller, and hence, the received power spectral density increases improving the SINR. However, at the same time the number of interferers (i.e., BSs)

TABLE I
ASSUMED PARAMETER FOR THE SIMULATION.

| Parameter | Value |
|---|---|
| Center frequency | 3.6 GHz and 26 GHz |
| Channel bandwidth | 50 MHz (for 3.6 GHz)<br>50 MHz and 200 MHz (for 26 GHz) |
| BS transmission power | 24 dBm |
| Mobile terminal (MT)<br>max transmission power<br>min transmission power | <br>23 dBm<br>$-40$ dBm |
| Receiver noise figure | 12 dB (BS), 9 dB (MT) |
| BS antenna gain<br>beamforming<br>omni | <br>23 dBi<br>5 dBi |
| Mobile terminal antenna gain | 0 dBi |
| Antenna heights<br>BS<br>mobile terminal | <br>3 m<br>1 m |
| Maximum spectral efficiency<br>(DL: 256 QAM, 2 streams)<br>(UL: 256 QAM, 1 stream) | <br>14.2 bps/Hz<br>7.1 bps/Hz |
| Path loss compensation factor ($\alpha$) | 0.8 |
| Number of users | 10 (downlink) , 10 (uplink) |

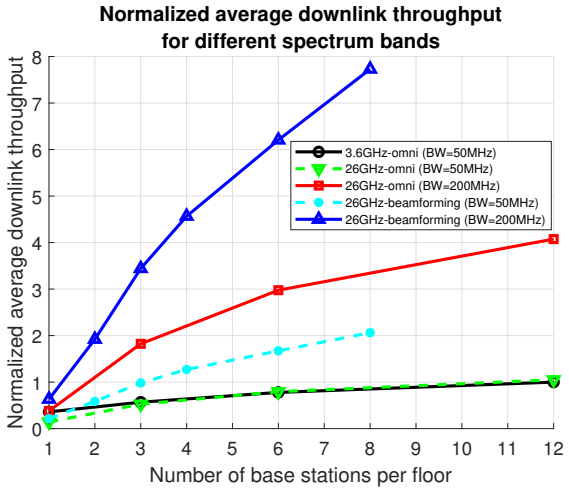


Fig. 2. Normalized average downlink throughput versus the number of BSs for 3.6 GHz and 26 GHz bands.

increases and the coupling losses towards the interfering BSs become smaller. As a result, the level of the DL inter-cell interference increases, making the DL more interference-limited. In all, network densification improves the DL SINR for noise-limited users, while it reduces the DL SINR for interference-limited users. Another benefit from network densification is the reduced number of simultaneously served users per BS, which means that the users are scheduled more often resulting in an improved average user throughput as in (9). Results in Fig. 2 indicate that even though the network densification can have both positive and negative impacts on the DL SINRs, the overall impact on the average user throughputs is positive due to the reduced BS loads.

Next we study the impact of center frequency on the DL performance. We compare the performance of a network operating in 3.6 GHz to the performance of a network operating in 26 GHz, assuming omnidirectional BS antennas and a

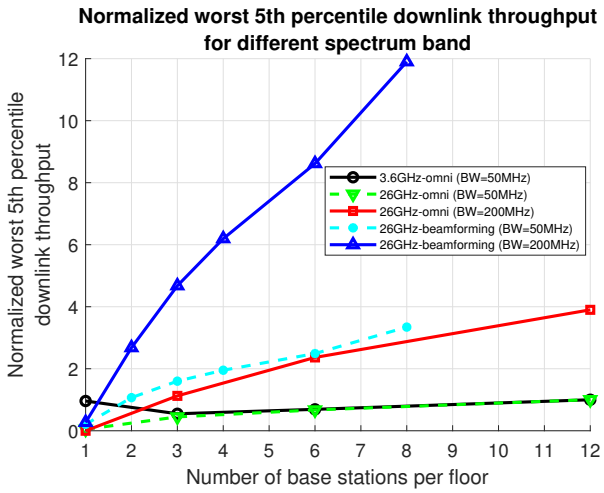


Fig. 3. Normalized worst 5th percentile throughput downlink throughput versus the number of BSs for 3.6 GHz and 26 GHz bands.

channel bandwidth equal to 50 MHz. Results show that when the BS density is low, i.e., when the DL SINR is noise-limited, the average and cell-edge throughputs observed in the 3.6 GHz band are slightly higher compared to the 26 GHz band. The DL performance differences for the noise-limited deployments are due to the quite large coupling loss differences between the two frequency bands. More specifically, as indicated by (2) the coupling losses in the 26 GHz band are approximately $17 - 22$ dB higher compared to the 3.6 GHz band. However, as the BS density increases, the network is becoming more interference-limited, which means that the coupling losses have a smaller impact on the DL SINRs, and further on the DL user throughputs. Thus, in the end the DL performance will become very similar for both frequency bands.

Next we investigate the impact of channel bandwidth on the DL performance as shown in Fig. 2 and Fig. 3, assuming deployment alternatives in the 26 GHz band with omnidirectional BS antennas. As the channel bandwidth increases from 50 MHz to 200 MHz, the received power spectral density becomes lower, resulting in a lower DL SINR for noise-limited deployments, and hence, a lower spectral efficiency. However, at the same time the average user throughputs benefit from the increased channel bandwidth ($\beta$), as indicated by (9). The obtained results show that even the noise-limited sparse deployments benefit from the increased channel bandwidth, indicating that the positive impact of increased channel bandwidth outweighs the negative impact of reduced spectral efficiency. In case of the more interference-limited dense deployments, the increased channel bandwidth has only a small impact on the DL SINR, and therefore, a four-fold increase in the channel bandwidth results in a nearly four-fold increase in the observed DL throughputs.

Finally, we analyze the impact of beamforming on the average and cell-edge DL throughputs in the 26 GHz band, as depicted in Fig. 2 and Fig. 3. The results show that the average and cell-edge throughputs with beamforming are considerably higher than with omnidirectional BS antennas. For the noise-

limited case, beamforming helps to reduce the coupling losses compared to the deployments with omnidirectional BS antennas. Thus, beamforming increases the DL throughputs by improving the signal-to-noise-ratio (SNR) of the users. When the network is interference-limited, the use of beamforming reduces both the coupling losses and in particular the level of the DL inter-cell interference. This is due to the fact that with beamforming the users do not see all the active BSs as effective DL interferers, because the active beams are quite often pointing away from the victim users. As a result, the use of beamforming helps to significantly improve the DL throughputs.

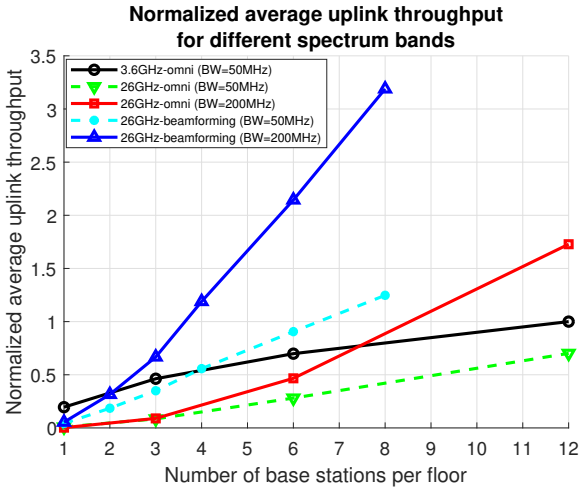


Fig. 4. Normalized average downlink throughput versus the number of BSs for 3.6 GHz and 26 GHz bands.

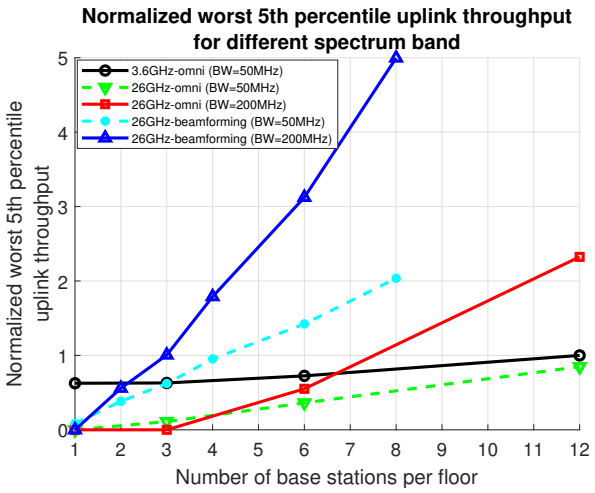


Fig. 5. Normalized worst 5th percentile throughput downlink throughput versus the number of BSs for 3.6 GHz and 26 GHz bands.

Fig. 4 shows the normalized average UL throughput and Fig. 5 shows the normalized cell-edge UL throughput versus BS density for different deployment alternatives. Similar to the DL, the results are normalized with respect to the deployment with 12 BSs in the 3.6 GHz band.

Results show that when the BS density increases the UL throughputs become higher. There are two main reasons for the improved UL performance as a result of network densification. The received UL power target $P_b^0$ can be increased together with the reduced coupling losses between the mobile terminals and the serving BSs. For example, we have observed that in case of the 3.6 GHz band the value of $P_b^0$ can be increased from $-133$ dBm to $-120$ dBm when the number of BSs is increased from 1 to 12. As a result of the increased $P_b^0$, the UL SNR is improved, enabling the use of higher modulation and coding schemes. However, similar to the DL, the level of UL inter-cell interference increases as a function of the increased BS density, due to the increased number of interfering mobile terminals, the increased $P_b^0$ values, and the reduced coupling losses between the interfering mobile terminals and the victim BSs. Hence, the network becomes more interference-limited as the BS density increases, reducing the benefits achieved by increasing the value of $P_b^0$. Second main reason explaining the improved UL performance is the reduced number of simultaneously active users per BS as a function of the increased BS density. As a result, the users can be scheduled more often, which directly improves the average user throughputs.

To evaluate the impact of center frequency on the UL performance, we compare the results for the 3.6 GHz and the 26 GHz band, assuming omnidirectional BS antennas and channel bandwidth equal to 50 MHz for both of them. The results show that both the average and the cell-edge UL throughputs in the UL are higher in the 3.6 GHz band compared to the 26 GHz for all the evaluated BS densities. These performance differences result from the higher coupling losses between the mobile terminals and the serving BSs, and consequently, lower $P_b^0$ values applied for the 26 GHz band. For this particular case, the applied $P_b^0$ values are 17 dB lower for the 26 GHz band compared to the 3.6 GHz band, which corresponds to the coupling loss difference equal to 22 dB (for NLOS links) and path loss compensation factor equal to 0.8. Due to the lower $P_b^0$ values in the 26 GHz band, the users experience lower UL SINR values, resulting in considerably worse UL throughputs in particular for the noise-limited deployments. In case of the more interference-limited dense deployments, the impact of reduced $P_b^0$ on the UL SINR becomes smaller, but there is still a clear performance difference in favor of 3.6 GHz band.

When it comes to the impact of channel bandwidth on the UL performance, it is important to note that the applied $P_b^0$ values have to be scaled accordingly in order to maintain the same total transmission power levels for the mobile terminals. Hence, if the channel bandwidth is increased from 50 MHz to 200 MHz, the applied $P_b^0$ values have to be reduced by 6 dB. As a result of the lowered $P_b^0$ values, the UL SINRs become worse. If the network is noise-limited, the SINR is reduced by the same amount as the bandwidth is increased (i.e., by 6 dB in this case), while for the more interference-limited deployments the SINR is reduced somewhat less. From the average user throughput point of view, there is a tradeoff between the increased channel bandwidth and the reduced SINR (i.e., the reduced spectral efficiency). However, as indicated by the obtained results, it is clearly beneficial to use a wider channel bandwidth, in particular

when the network is dense enough to provide sufficient UL coverage ($\mathrm{SINR} > -10$ dB) throughout the evaluated floor area. As can be noticed, the average UL throughput with 12 BSs in the 26 GHz band is approximately 2.5 times as high as the corresponding throughput in the 3.6 GHz band.

Finally, beamforming reduces the coupling losses between the mobile terminals and the serving BSs, which allows higher $P_b^0$ values to be applied. For example, in these evaluations the difference compared to deployments with omnidirectional antennas is in the range of $6 - 8$ dB. As a result of the higher $P_b^0$ values, the UL SINRs and further the UL throughputs are improved. Similar to the DL, the use of beamforming reduces the level of inter-cell interference as well. However, since UL in 26 GHz band is considerably less interference-limited compared to DL, the additional gain due to the reduced inter-cell interference is fairly small compared to the gain due to the increased $P_b^0$ values.

In the sequel, we summarize the above evaluated performances by comparing each deployment alternative by comparing the minimum number of BSs required to achieve a similar performance both in terms of average and cell-edge throughput. By inspecting Fig. 2 and Fig. 3, we can see that the center frequency does not have any remarkable impact on the DL performance of an interference-limited dense deployment. However, it does have a clear negative impact on the UL performance (see Fig. 4 and Fig. 5). This is due to the fact that as a result of the applied UL power control with fractional path loss compensation the UL is less interference-limited compared to the DL, and hence, the impact of the coupling loss difference between the evaluated bands is more visible. That is also the reason why the DL benefits much more from the increased channel bandwidth compared to the UL. Furthermore, it could also be seen that beamforming is highly beneficial for the performance of both the DL and the UL, in particular when combined with the additional channel bandwidth.

## IV. Conclusion

In this paper, we have focused on local indoor 5G networks and investigated the suitability of the two 5G bands, namely 3.6 GHz and 26 GHz bands, for their operations. We have used system level simulations to evaluate the performance of alternative deployments for a single indoor local 5G micro operator network in terms of the average and cell-edge throughputs in the DL and UL. We have observed that the average and cell-edge throughputs in the DL and UL of these two bands can be increased, by increasing the base station density. Furthermore, we have seen that the center frequency does not have any remarkable impact on the DL performance unless the network is noise-limited. However, in the case of UL the performance in the 26 GHz band suffers from the considerably higher coupling losses between the BSs and the mobile terminals. We have also quantified how the network performance in 26 GHz band can be considerably improved by applying both wider channel bandwidths and beamforming. Future work is needed to evaluate the performance of 5G micro operator networks in indoor-to-outdoor and outdoor deployments.

## References


[1] 5GPP, "5G empowering vertical industries: roadmap paper," Tech. Rep., The 5G infrastructure public private partnership, 2016.

[2] Ericsson AB, "5G systems enabling transformation of industry and society," Tech. Rep., Jan. 2017.

[3] ETSI, "Feasibility study on temporary spectrum access for local high-quality wireless networks ETSI TR 103 588 version 1.1.1.)," Tech. Rep., The European Telecommunications Standards Institute, 2018.

[4] M. D. P. Guirao, A. Wilzeck, A. Schmidt, K. Septinus, and C. Thein, "Locally and temporary shared spectrum as opportunity for vertical sectors in 5G," *IEEE Network*, vol. 31, no. 6, pp. 24–31, Nov. 2017.

[5] J. Zander, "Beyond the ultra-dense barrier: Paradigm shifts on the road beyond 1000x wireless capacity," *IEEE Trans. Wireless Commun.*, vol. 24, no. 3, pp. 96–102, 2017.

[6] M. Matinmikko-Blue, M. Latva-aho, P. Ahokangas, S. Yrjölä, and T. Koivumäki, "Micro operators to boost local service delivery in 5G," *Wireless Pers. Commun., Springer*, vol. 95, no. 1, pp. 69–82, 2017.

[7] M. G. Kibria, G. P. Villardi, K. Nguyen, W. S. Liao, K. Ishizu, and F. Kojima, "Shared spectrum access communications: A neutral host micro operator approach," *IEEE J. Select. Areas Commun.*, vol. 35, no. 8, pp. 1741–1753, Aug. 2017.

[8] M. Matinmikko-Blue, M. Latva-aho, P. Ahokangas, and V. Seppänen, "On regulations for 5G: Micro licensing for locally operated networks," *Els. Teleco. Policy*, Sept. 2017.

[9] P. Anker, "From spectrum management to spectrum governance," *Els. Teleco. Policy*, vol. 41, no. 5, pp. 486 – 497, Sept. 2017.

[10] K. B. S. Manosha, M. Matinmikko-Blue, and M. Latva-aho, "Framework for spectrum authorization elements and its application to 5G micro-operators," in *Internet of Things Business Models, Users, and Networks*, Nov. 2017, pp. 1–8.

[11] K. Hiltunen, M. Matinmikko-Blue, and M. Latva-aho, "Impact of interference between neighbouring 5G micro operators," *Wireless Pers. Commun., Springer*, vol. 100, no. 1, pp. 127–144, May 2018.

[12] European Commission, "Strategic spectrum roadmap towards 5G for Europe, RSPG second opinion on 5G networks," Tech. Rep., Radio Spectrum Policy Group RSPG, RSPG18-005, 2018.

[13] 3rd Generation Partnership Project (3GPP); Technical Specification Group Radio Access Network, "Study on channel model for frequencies from 0.5 GHz to 100 GHz (3G TR 38.901 version 14.1.1.)," Tech. Rep., 3rd Generation Partnership Project (3GPP), 2017.